Non-Negligible Diffusio-Osmosis Inside an Ion Concentration Polarization Layer

Inhee Cho,[1] Wonseok Kim,[1] Junsuk Kim,[1] Ho-Young Kim,[2,3,4] Hyomin Lee,[1,3,*] and Sung Jae Kim[1,4,5,†]
[1]*Department of Electrical and Computer Engineering, Seoul National University, Seoul 08826, South Korea*
[2]*Department of Mechanical and Aerospace Engineering, Seoul National University, Seoul 08826, South Korea*
[3]*Institute of Advanced Machines and Design, Seoul National University, Seoul 08826, South Korea*
[4]*Big Data Institute, Seoul National University, Seoul 08826, South Korea*
[5]*Interuniversity Semiconductor Research Center, Seoul National University, Seoul 08826, South Korea*
(Received 28 February 2016; published 20 June 2016)

The first experimental and theoretical evidence was provided for the non-negligible role of a diffusio-osmosis in the ion concentration polarization (ICP) layer, which had been reported to be in a high Peclet number regime. Under the assumption that the hydrated shells of cations were stripped out with the amplified electric field inside the ICP layer, its concentration profile possessed a steep concentration gradient at the stripped location. Since the concentration gradient drove a strong diffusio-osmosis, the combination of electro-osmotic and diffusio-osmotic slip velocity had a form of an anomalous nonmonotonic function with both a single- and multiple-cationic solution. A direct measurement of electrolytic concentrations around the layer quantitatively validated our new investigations. This non-negligible diffusio-osmotic contribution in a micro- and nanofluidic platform or porous medium would be essential for clarifying the fundamental insight of nanoscale electrokinetics as well as guiding the engineering of ICP-based electrochemical systems.

DOI: 10.1103/PhysRevLett.116.254501

With the aid of recent developments of nanotechnology, the fundamental studies of electrokinetics with the micro- and nanofluidic interface have been actively reported both on the fundamental theories and engineering applications [1–3]. One of the most exciting features in the nanoscale electrokinetics is an ion concentration polarization (ICP) phenomenon that describes the significant concentration gradient formed at both ends of the nanochannel (or nanoporous membrane) under direct current (dc) bias [4–7]. Several seminal experimental or theoretical works have reported on the underlying physicochemical hydrodynamics inside the ICP layer. In particular, the in-depth understanding of an ion depletion zone at the anodic side of a cation-selective membrane became the unprecedentedly active research field, since the multiscale couplings of an extremely low concentration distribution [8,9], an amplified electric field [10,11], and an electroconvection [12–15] or surface conduction [16–18] at the micronano interface were tightly involved. While the classical theory has considered a diffusion and a drift ionic transportation to predict a linear concentration gradient near the membrane [19], the visualization of strong vortical flow inside the ion depletion zone has proved the significant role of the electroconvections [6] and the overlimiting conductance measurements with a confined microchannel structure unveiled the contribution of the surface conduction to the overlimiting current [17]. Therefore, the comprehensive understanding of the classical diffusion-limited theory as well as the newly investigated electroconvection and surface conduction were demanded for the complete picture of the ion depletion zone.

More importantly, the electrolyte concentration profile inside the ion depletion zone is one of the most essential fingerprints for the ICP phenomenon together with *I-V* responses (i.e., Ohmic, limiting, and overlimiting current), since it not only reflects the ion transportation through the membrane but also determines several important parameters for developing engineered ICP applications. Recently, a number of experimental and simulated demonstrations reported the basic structure of the profile [13,20–23]. While the classical diffusion limited theory suggested a linear concentration profile (i.e., diffusion layer) from the membrane to the bulk, the recent studies demonstrated that a strong convection was involved to produce the profile as the combination of the extended space charge layer, the mixing layer at a near-zero concentration, and the diffusion layer. From these publications, one would expect the monotonic function of the electric field so that the associated electrokinetic slip velocity inside the ion depletion zone should be monotonic as well.

In this work, the high-resolution electrokinetic slip velocity profiles along the ion depletion zone were measured by local trapping the vortices in microgrooves, leading to a nonmonotonic velocity peak that cannot be explained by the aforementioned studies. Under the assumption that the shells of cations were stripped out [24–28] with the amplified electric field inside the ICP layer, the mobility of the cation steeply increased over the threshold electric field, developing a stepwise concentration distribution. In the meantime, the nontrivial peak was attributed as the differential form of such stepwise concentration changes, which strongly drove the diffusio-osmotic contribution to the local slip velocity inside the ion depletion zone, while the diffusio-osmosis had been neglected in the system involving a strong convection (high

Peclet number regime). As tangible evidence, a direct measurement of extracted samples from the ion depletion zone using a mass spectrometry confirmed the non-negligible contribution of the diffusio-osmosis inside the ion depletion zone.

A polydimethylsiloxane microchip incorporated within a Nafion nanoporous membrane was fabricated as shown in Fig. 1(a). The main microchannel had microgrooves along each wall [see the inset of Fig. 1(a)]. The details of the fabrication steps and the geometrical information are given in Supplemental Material [29]. The grooves were able to trap the flow trackers (diameter of canola oil droplets = ~2 um) and they rotated only inside the grooves with an angular velocity that was proportional to the local electrokinetic slip velocity because of the low surface charge density of oil droplets. Fingerprinted I-V responses were measured for various microchannel heights and the overall I-V behaviors were identical at the height over 200 um with 20×20 um square grooves, eliminating the cross talk between each grooved wall. See Supplemental Material [29] for this test.

According to the mean field model with constant mobility, the magnitude of the rotational speed should monotonically decrease [being fastest near the membrane and slowest near the boundary of ICP layer as shown in Fig. 1(b)i.], since the electric field should be a monotonic function. However, the speeds were measured with a high-speed camera and the fastest slip velocity appeared in the middle of the ICP layer as a schematic diagram shown in Fig. 1(b)ii. See the actual experimental video in Supplemental Material [29]. The speeds were quantified as shown in Figs. 2(a) and 2(b) for LiCl and NaCl 1 mM solution, respectively. The same experiments with lower bulk concentrations (0.1 and 0.01 mM) for stronger ICP formation were conducted and it was found that the locations of peak were measured to be identical, since the system fell into the surface-charge-governed regime [32] (*i.e.*, independent from bulk concentration) with the same length of ICP layer. See the details in Supplemental Material [29]. The mathematical function of curve fitting was arbitrarily chosen just for the clear visualization of the experimental plot. See Supplemental Material [29] for the fitting equations and fitting parameters. The emergence of this nontrivial velocity distribution far from the theoretical prediction has to be differently explained only with the electro-osmotic flow. Note that the minimum resolution of the measurement was 20 um due to the fabrication limitation of microgrooves.

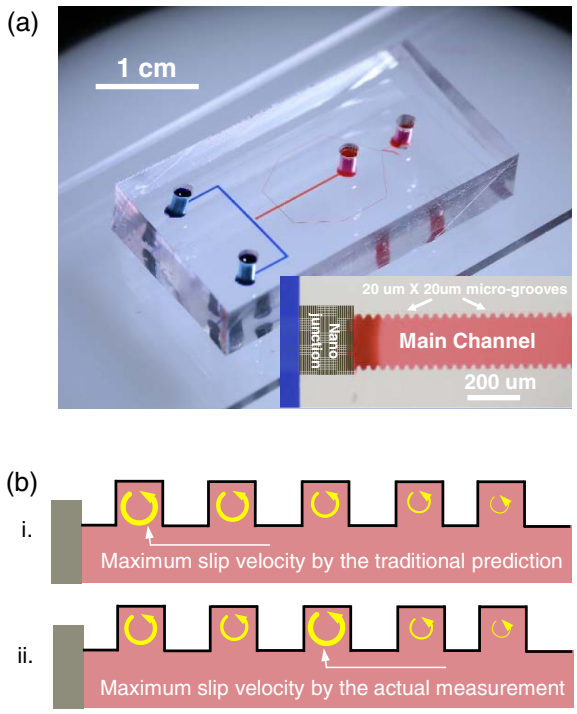

FIG. 1. (a) An image of the micro- and nanofluidic device that has microgrooves along the main microchannel. Numbers in the inset point to the numbering of each groove. (b) Schematic diagrams of the trapped vortices in the microgrooves by (i.) the mean field model with constant mobility and (ii.) the actual measurement. The thickness of arrows indicates the magnitude of the rotational speeds.

Although the mobility of ions has usually been treated as a constant quantity, the mobility can be modified by the fact that the extremely high electric field can strip the hydrated shell of the ionic species [24–28]. Because of the reduced diameter by the stripped shell, the mobility of the ion should become faster based on the Stokes-Einstein relationship (mobility is inversely proportional to diameter). Thus, the hypothetical mobility change is shown in the first plot of Fig. 2(c). [The plots in Fig. 2(c) were only for the case of LiCl.] The mobility altered at a threshold electric field. According to previous literature [33], the mobility of Li^+ of the dehydrated state was set six times higher than that of the hydrated state. Typical intensity of the threshold electric field was reported to be $\mathrm{MV/m} \sim \mathrm{GV/m}$ in a gas phase [34], but the value reduced to few $0.01\ \mathrm{MV/m} \sim 0.01\ \mathrm{GV/m}$ in a liquid phase due to the large permittivity of liquid ($\varepsilon_{\mathrm{gas}} \approx 1$ and $\varepsilon_{\mathrm{water}} \approx 80$) and this magnitude was achievable in the ICP layer by the amplified electrokinetic response. Direct experimental evidence for the induced high electric field inside the ICP layer was previously reported by our group [10,21]. In those papers, we periodically installed metal microelectrodes inside a microchannel and measured electric fields directly both inside and outside the ICP layer. Those reports quantitatively showed that the high electric field (~0.1 MV/m) was induced only inside the ICP layer, while the field was the same as the externally applied electric field ($\sim 3,000$ V/m) outside the ICP layer. In addition, other groups also showed that electric field generated inside the ICP layer was amplified over one hundred times more than that outside the ICP layer using theoretical analysis as well [35,36].

Using the field-induced mobility change of Li^+, numerically simulated cation concentration had the Heaviside distribution inside the ion depletion zone as shown in the second plot of Fig. 2(c). The threshold electric field as a modeling parameter was arbitrarily chosen to describe the

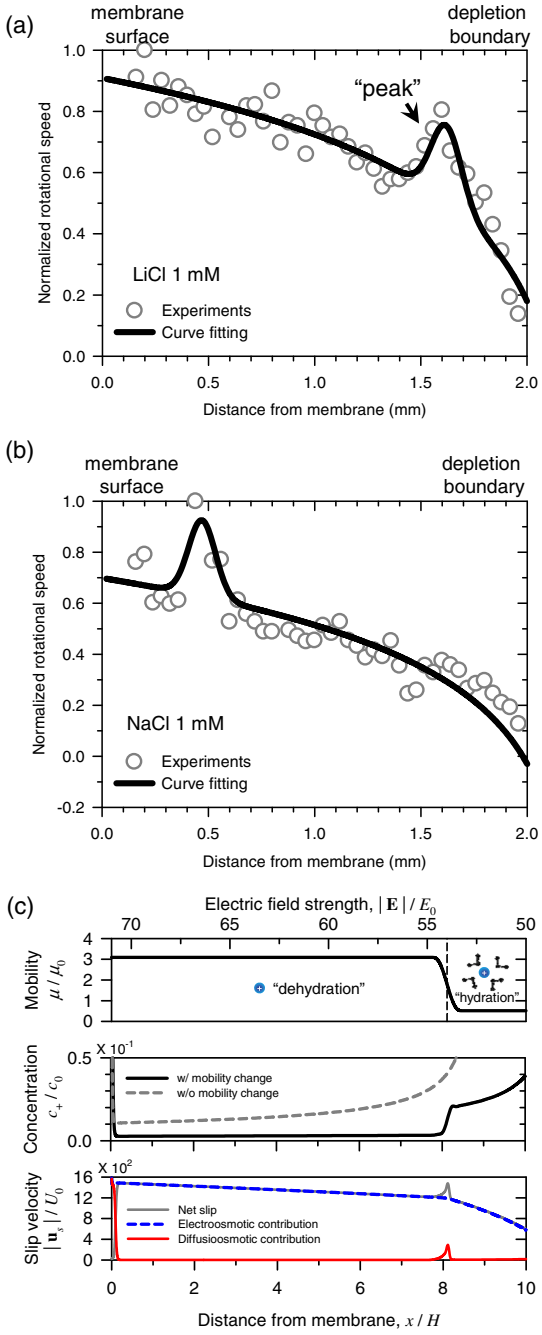

FIG. 2. Experimentally measured rotational speeds of the flow tracker inside the microgrooves as a function of the distance inside the ICP layer with the (a) LiCl and (b) NaCl solution. The rotational speeds were normalized by the experimentally measured maximum speed. The curve fitting was plotted with arbitrarily chosen functions. (c) Plots for the mobility change of Li^+ as a function of an applied electric field, the concentration distribution of Li^+, and the slip velocities as a function of distance from the membrane. The concentration distribution and slip velocity were numerically obtained. The normalized parameters were as follows: E_0 is the thermal voltage scale electric field (i.e., $RTF^{-1}L^{-1}$, where R is the gas constant, T is the absolute temperature, F is the Faraday constant, and L is the length of microchannel), μ_0 is the mobility of Cl^-, c_0 is the bulk concentration, and U_0 is the thermal voltage scale velocity (i.e., $\varepsilon\eta^{-1}L^{-1}R^2T^2F^{-2}$, where ε is the electric permittivity of water and η is the dynamic viscosity of water), respectively.

location of the velocity peak inside the ICP layer. This concentration distribution coincided with the previous results by measuring a local electric conductivity in which the concentration profile inside the ion depletion zone was the Heaviside function [21]. This peculiar distribution has not been predicted by any mean field model before. The concentration profile without the field-induced mobility change (gray dashed line) was a monotonically increased function shown in the second plot of Fig. 2(c).

From the fundamental electrokinetic theory [37–39], the diffusio-osmosis as well as the electro-osmosis is able to generate the effective slip velocity at the substrate wall in the electrochemical system. See Supplemental Material [29] for the detailed equations. Since the driving force of the diffusio-osmosis is the gradient of chemical potential that is defined by the logarithm of the local concentration ($\nabla \ln(c/c_{\mathrm{ref}}) = \nabla c/c$), one can expect the sharp driving force around the steplike change of the concentration at $x/H = \sim 8$ in the case of Li^+. Consequently, the strong diffusio-osmotic slip (red solid line) contributed to the net slip velocity (gray solid line) in addition to the electro-osmotic slip velocity (blue dash line) as shown in the third plot of Fig. 2(c). Mathematically, $\nabla f/f$ where f is an arbitrary sigmoidal function also has the peak shape such as the Gaussian function. Except for $x/H = \sim 8$, the diffusio-osmotic contribution to the slip velocity is near 0, since there is no significant concentration gradient in this region. Note that the steep changes around $x/H = 0$ resulted from the abundant counterions (c_+) adjacent to the negatively charged membrane surface due to the electrical double layer (EDL) where the counterions were gathered to neutralize the surface charge. This counterion concentration at $x/H = 0$ was called the Donnan equilibrium concentration (N) of which value was set to be much larger than the bulk concentration (c_0) for the case of the ideal selective membrane. One usually sets the value more than $2c_0$ [40,41]. When the ICP layer was developed near the membrane, c_+ in the EDL asymptotically decreased from the Donnan concentration to zero concentration [35,36]. Since the thickness of the EDL is usually 0.3 nm–1 um for 1 M–10^{-7} M electrolytic solution and it leads considerably steep concentration gradients, the diffusio-osmotic contribution [red line in Fig. 2(c)] steeply decreased (the diffusio-osmosis is proportional to the concentration gradient) near $x/H = 0$.

For a multiple-cationic mixture of LiCl and NaCl, we experimentally confirmed that the local slip velocity has two peaks as shown in Fig. 3(a). This interesting observation resulted from the hypothetical electric field-induced mobility change as well. As shown in the first plot of Fig. 3(b), each cation has different specific threshold electric fields. The values were empirically chosen for each cation by observing that the peak of Na^+ appeared closer to the membrane surface than that of Li^+ [see Figs. 2(a) and 2(b)]. In the meantime, the mobility of Li^+ and Na^+ elevated six and four times, respectively [33]. These combined effects led to the steplike changes of the cation concentrations at their specific locations [$x/H = \sim 3$ and ~ 7 for Na^+ and Li^+, respectively, in the

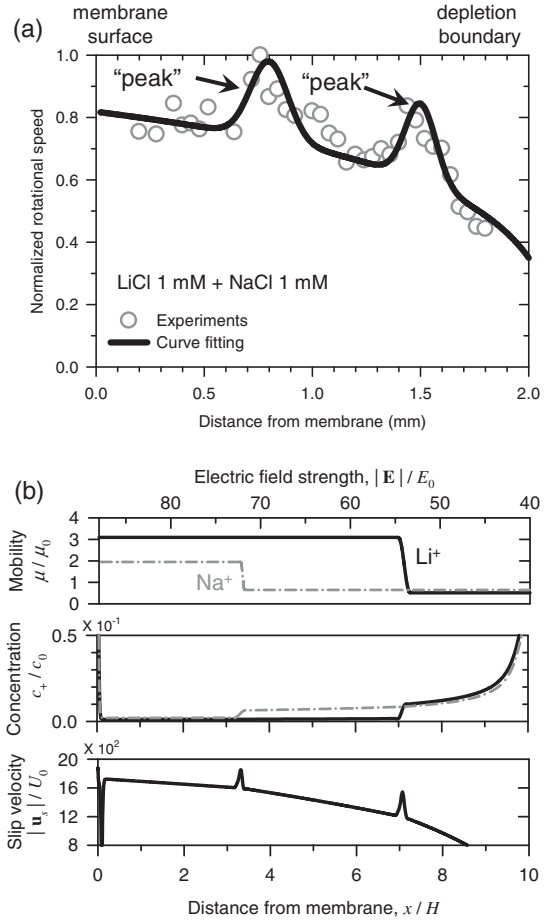

FIG. 3. (a) Experimentally measured rotational speeds of the flow tracker inside the microgrooves with a multiple-cationic mixture of LiCl and NaCl solution. (b) Plots for the mobility changes of Li^+ and Na^+ as a function of an applied electric field, the concentration distribution of Li^+ and Na^+, and the slip velocities as a function of distance from the membrane. The concentration distribution and slip velocity were numerically obtained.

second plot of Fig. 3(b)] and the sharp peaks of the slip velocity at the designated locations [the third plot of Fig. 3(b)]. Therefore, the model considering the diffusio-osmosis and the field-induced mobility change successfully illustrated the appearance of anomalous velocity peaks not only with a single cationic solution but also a multiple-cationic mixture.

The simulation results of each cationic concentration [the second plot of Fig. 3(b)] suggest that the Na^+ ion predominates in the range of $0 < x/H < 7$ and Li^+ slightly dominates over Na^+ in the range of $7 < x/H < 10$ so that there should be the inversion of the concentration values along the ICP layer. Note that the numerical model without the field-induced mobility change suggests that the concentration of Li^+ is always (slightly) higher than that of Na^+. See the Supplemental Material [29]. In order to confirm the existence of the inversion point, a five-branched micro- and nanofluidic device was fabricated as shown in Fig. 4(a). The mixture of LiCl (20 mM) and NaCl (20 mM) was pumped across the ion depletion zone and most of the ions were expelled from the zone. 20 mM of samples were used in this experiment because the concentration above 20 mM guarantees the reliable measurement at outlet 1, which is the closest outlet from the membrane, while the slip velocity measurement experiments were conducted with 1 mM of samples. Since the sample was continuously injected, the deionized samples were constantly collected at each branch so that the concentrations around the ICP layer were able to be discretized. See Supplemental Material [29] for the experimental details. Inductively coupled plasma optical emission spectrometry was employed to quantify the concentration of collected samples as shown in Fig. 4(b). Remarkably, the concentrations of Na^+ were higher than those of Li^+ only at outlets 1 and 2, while the quantities were inversed at outlets 3–5. Most importantly, the model without the field-induced mobility change (see Supplemental Material [29]) is incapable of describing the inversion of concentration inside the ICP layer, since the concentration of Li^+ is always higher than that of Na^+ in the whole region inside the ICP layer. Thus, this result is strong direct evidence for our model of the diffusio-osmosis and the field-induced mobility change.

The diffusio-osmosis has been believed to play a significant role only for the case of a zero Peclet number limit [42]; i.e., the convection transport is negligible compared to the diffusion transport. Moreover, since the ICP phenomenon possessed a strong convective (or vortical) flow field [6,14], one always neglected the effect of the diffusio-osmosis in the

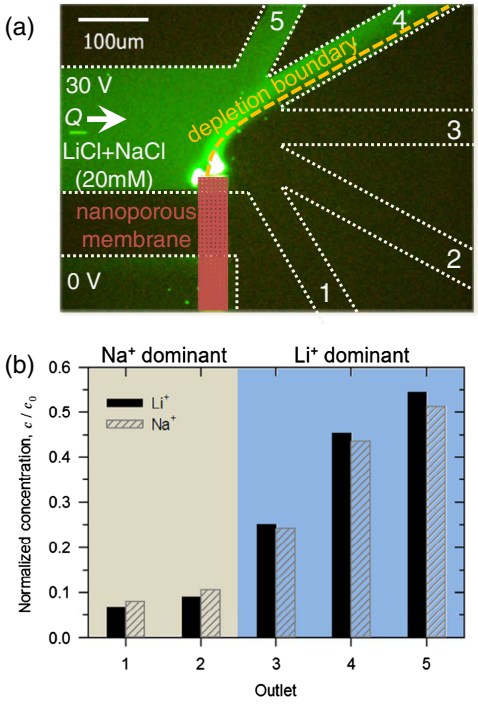

FIG. 4. (a) An experimental demonstration of collecting the discretized samples from the ICP layer using the five-branched micro- and nanofluidic device. (b) A quantitative concentration measurement of each cation, showing that the dominance was inversed between outlet 2 and 3.

ICP phenomenon. However, we demonstrated, for the first time, the *in situ* measurement of the local slip velocity inside the ICP layer as the nonmonotonic function that cannot be fully elucidated by the previous insight. The formation of the slip velocity peaks within the ICP layer was attributed to the contribution of the diffusio-osmosis, since the local amplified electric field generated a steep concentration gradient (which is the driving force of the strong diffusio-osmosis) by the hypothesis of the field-induced mobility change. This result led to the concentration profile in a form of the Heaviside function and the peak of the slip velocity inside the ICP layer. Important features of these findings were validated by the direct measurement of collected samples within the ICP layer. Therefore, the main conclusion from this Letter is that the diffusio-osmosis is non-negligible even in a high Peclet number limit depending on the hydrated status of major carriers. Consequently, further studies should be reserved for investigating the effect of diffusio-osmosis on the ion transportation through the membrane in addition to the diffusion, the drift, and the electroconvection transportation. A clear understanding of such ion transportation mechanisms inside the ICP layer in micro- and nanofluidic platform or porous media are essential, not only for developing the fundamental insight of nanoscale electrokinetics, but also for guiding the engineering of ICP-based electrochemical systems, such as the ion separator, fuel cells, batteries, and electrodesalination systems.

This work was supported by the National Research Foundation of Korea (Grants No. CISS-2011-0031870, No. 2012-0009563, No. 2014-048162, and No. 2016R1A1A1A05005032) and the Korean Health Technology RND project (Grants No. HI13C1468 and No. HI14C0559). All authors acknowledge the support from the BK21+ program of Creative Research Engineer Development IT, Seoul National University.

I. C. and W. K. contributed equally to this work.

*naonfluidics@snu.ac.kr
†gates@snu.ac.kr

[1] R. B. Schoch, J. Han, and P. Renaud, Rev. Mod. Phys. **80**, 839 (2008).
[2] J. C. T. Eijkel and A. van den Berg, Microfluid. Nanofluid. **1**, 249 (2005).
[3] R. Mukhopadhyay, Anal. Chem. **78**, 7379 (2006).
[4] R. F. Probstein, *Physicochemical Hydrodynamics: An Introduction* (Wiley-Interscience, New York, 1994).
[5] I. Rubinstein and L. Shtilman, J. Chem. Soc., Faraday Trans. 2 **75**, 231 (1979).
[6] S. J. Kim, Y.-C. Wang, J. H. Lee, H. Jang, and J. Han, Phys. Rev. Lett. **99**, 044501 (2007).
[7] T. A. Zangle, A. Mani, and J. G. Santiago, Chem. Soc. Rev. **39**, 1014 (2010).
[8] S. J. Kim, S. H. Ko, K. H. Kang, and J. Han, Nat. Nanotechnol. **5**, 297 (2010).
[9] G. Yossifon and H.-C. Chang, Phys. Rev. Lett. **101**, 254501 (2008).
[10] S. J. Kim, L. Li, and J. Han, Langmuir **25**, 7759 (2009).
[11] M. K. Urtenov, A. M. Uzdenova, A. V. Kovalenko, V. V. Nikonenko, N. D. Pismenskaya, V. I. Vasil'eva, P. Sistat, and G. Pourcelly, J. Membr. Sci. **447**, 190 (2013).
[12] B. Zaltzman and I. Rubinstein, J. Fluid Mech. **579**, 173 (2007).
[13] X. Jin, S. Joseph, E. N. Gatimu, P. W. Bohn, and N. R. Aluru, Langmuir **23**, 13209 (2007).
[14] S. M. Rubinstein, G. Manukyan, A. Staicu, I. Rubinstein, B. Zaltzman, R. G. H. Lammertink, F. Mugele, and M. Wessling, Phys. Rev. Lett. **101**, 236101 (2008).
[15] V. S. Pham, Z. Li, K. M. Lim, J. K. White, and J. Han, Phys. Rev. E **86**, 046310 (2012).
[16] E. V. Dydek, B. Zaltzman, I. Rubinstein, D. S. Deng, A. Mani, and M. Z. Bazant, Phys. Rev. Lett. **107**, 118301 (2011).
[17] S. Nam, I. Cho, J. Heo, G. Lim, M. Z. Bazant, D. J. Moon, G. Y. Sung, and S. J. Kim, Phys. Rev. Lett. **114**, 114501 (2015).
[18] C. P. Nielsen and H. Bruus, Phys. Rev. E **90**, 043020 (2014).
[19] V. G. Levich, *Physico-Chemical Hydrodynamics* (Prentice-Hall, London, 1962).
[20] I. Rubinstein and B. Zaltzman, Phys. Rev. E **80**, 021505 (2009).
[21] S. J. Kim, S. H. Ko, R. Kwak, J. D. Posner, K. H. Kang, and J. Han, Nanoscale **4**, 7406 (2012).
[22] R. Dhopeshwarkar, R. M. Crooks, D. Hlushkou, and U. Tallarek, Anal. Chem. **80**, 1039 (2008).
[23] I. Rubinstein and B. Zaltzman, Phys. Rev. E **81**, 061502 (2010).
[24] C. Y. Lee, W. Choi, J. H. Han, and M. S. Strano, Science **329**, 1320 (2010).
[25] K. Kadota, A. Shimosaka, Y. Shirakawa, and J. Hidaka, J. Nanopart. Res. **9**, 377 (2007).
[26] J. Dzubiella and J.-P. Hansen, J. Chem. Phys. **122**, 234706 (2005).
[27] X. Wu, L. Lu, Y. Zhu, Y. Zhang, W. Cao, and X. Lu, Fluid Phase Equilib. **353**, 1 (2013).
[28] W. Choi, Z. W. Ulissi, S. F. E. Shimizu, D. O. Bellisario, M. D. Ellison, and M. S. Strano, Nat. Commun. **4**, 2397 (2013).
[29] See Supplemental Material at http://link.aps.org/supplemental/10.1103/PhysRevLett.116.254501 for the experimental details, additional experiments, and detailed theoretical formulations, which includes Refs. [30,31].
[30] I. Rubinstein and B. Zaltzman, Adv. Colloid Interface Sci. **159**, 117 (2010).
[31] D. C. Prieve, J. L. Anderson, J. P. Ebel, and M. E. Lowell, J. Fluid Mech. **148**, 247 (1984).
[32] D. Stein, M. Kruithof, and C. Dekker, Phys. Rev. Lett. **93**, 035901 (2004).
[33] B. E. Conway, *Ionic Hydration in Chemistry and Biophysics* (Elsevier, New York, 1981).
[34] P. J. Taylor, A. O. Ntukogu, S. S. Metcal, and L. B. Rogers, Separation science **8**, 245 (1973).
[35] A. S. Khair, Phys. Fluids **23**, 072003 (2011).
[36] M. A. K. Urtenov, E. V. Kirillova, N. M. Seidova, and V. V. Nikonenko, J. Phys. Chem. B **111**, 14208 (2007).
[37] S. S. Dukhin, Adv. Colloid Interface Sci. **35**, 173 (1991).
[38] H. J. Keh and H. C. Ma, Langmuir **21**, 5461 (2005).
[39] J. L. Anderson, Annu. Rev. Fluid Mech. **21**, 61 (1989).
[40] C. L. Druzgalski, M. B. Andersen, and A. Mani, Phys. Fluids **25**, 110804 (2013).
[41] Y. Green and G. Yossifon, Phys. Rev. E **87**, 033005 (2013).
[42] R. A. Rica and M. Z. Bazant, Phys. Fluids **22**, 112109 (2010).